J|A|C|S
ARTICLES
Published on Web 02/16/2007

An IR Study of Protonation Changes Associated with Heme−Heme Electron Transfer in Bovine Cytochrome *c* Oxidase

Masayo Iwaki and Peter R. Rich*

Contribution from the Glynn Laboratory of Bioenergetics, Department of Biology, University College London, Gower Street, London WC1E 6BT, United Kingdom

Received October 31, 2006; E-mail: prr@ucl.ac.uk

Abstract: IR changes caused by photolysis of CO from the mixed valence form of bovine cytochrome *c* oxidase have been investigated over the pH/pD range 6−9.8. Band assignments were based on effects of H_2O/D_2O exchange and by comparisons with published IR data and crystallographic data. Changes arise both from CO photolysis and from subsequent reversed electron transfer from heme a_3 to heme *a*. This reversed electron transfer is known to have pH-independent and, above pH 8, pH-dependent components. The pH-independent component is associated with a trough around the 1742 cm^{-1} band attributable to one or more protonated carboxylic acids. Its peak position, but not extent, is pH-dependent, indicative of a titratable group with a p*K* of 8.2 whose acid form causes increased hydrogen bonding to the IR-detectable carboxylic group. A different protonatable group with p*K* above 9 controls the extent of the pH-dependent component. This phase is associated with perturbation of an arginine guanidinium that is most clearly observed as a trough at 1592 cm^{-1} after H/D exchange. It is suggested that this group, probably Arg-438 that is in close contact with propionate groups of both hemes and already proposed to be of functional significance, lowers the energy of the transient charge-uncompensated electron-transfer intermediate by changing the charge distribution in response to heme−heme electron transfer. No other IR signature of a titratable group that controls the extent of the pH-dependent phase is present, and it most likely arises from a nonphysiological deprotonation of the proximal water ligand of ferric heme a_3 at high pH that has been reported to exhibit a similar p*K*.

Introduction

Although many details of the atomic structure[1−4] and reaction cycle[5−7] of cytochrome *c* oxidase (C*c*O) are known, the specific chemistry that couples proton translocation to electron transfer and oxygen reduction remains unclear. Several proposals involve a pathway for proton translocation that is linked primarily to heme *a* redox changes.[8,9] However, others are based on an electrostatic model[10] that arose from empirical measurements of the necessity for charge neutralization within the binuclear center.[11,12] In this proposal, a proton to be translocated is electrostatically driven into a "trap site" in concert with electron transfer from heme *a* to the binuclear center.[10] Subsequent protonation of the binuclear center for oxygen chemistry results in charge imbalance and expulsion of the "trap" proton into the positive aqueous phase. Two recent reports[13,14] provide further support that this general model occurs, although the identities of the key protonatable residues, of which there are various possible candidates, remain unknown[15] (Figure 1).

The heme−heme electron-transfer step can be studied transiently in the forward direction by initiation of oxygen reduction by the fully reduced (FR) C*c*O with the "flow-flash" technique,[16,17] which, in combination with vis/UV,[18−20] electrometric,[14,21] and proton detection[13,22] methods in the microsecond

(1) Iwata, S.; Ostermeier, C.; Ludwig, B.; Michel, H. *Nature* **1995**, *376*, 660−669.
(2) Tsukihara, T.; Aoyama, H.; Yamashita, E.; Tomizaki, T.; Yamaguchi, H.; Shinzawa-Itoh, K.; Nakashima, R.; Yaono, R.; Yoshikawa, S. *Science* **1996**, *272*, 1136−1144.
(3) Svensson-Ek, M.; Abramson, J.; Larsson, G.; Törnroth, S.; Brzezinski, P.; Iwata, S. *J. Mol. Biol.* **2002**, *321*, 329−339.
(4) Tsukihara, T.; Shimokata, K.; Katayama, Y.; Shimada, H.; Muramoto, K.; Aoyama, H.; Mochizuki, M.; Shinozawa-Itoh, K.; Yamashita, E.; Yao, M.; Ishimura, Y.; Yoshikawa, S. *Proc. Natl. Acad. Sci. U.S.A.* **2003**, *100*, 15304−15309.
(5) Babcock, G. T. *Proc. Natl. Acad. Sci. U.S.A.* **1999**, *96*, 12971−12973.
(6) Wikström, M. *Biochim. Biophys. Acta* **2004**, *1655*, 241−247.
(7) Michel, H. *Biochemistry* **1999**, *38*, 15129−15140.
(8) Yoshikawa, S.; Muramoto, K.; Shinzawa-Itoh, K.; Aoyama, H.; Tsukihara, T.; Ogura, T.; Shimokata, K.; Katayama, Y.; Shimada, H. *Biochim. Biophys. Acta* **2006**, *1757*, 395−400.
(9) Papa, S.; Lorusso, M.; di Paola, M. *Biochim. Biophys. Acta* **2006**, *1757*, 428−436.
(10) Rich, P. R. *Aust. J. Plant Physiol.* **1995**, *22*, 479−486.
(11) Mitchell, R.; Mitchell, P.; Rich, P. R. *Biochim. Biophys. Acta* **1992**, *1101*, 188−191.
(12) Mitchell, R.; Rich, P. R. *Biochim. Biophys. Acta* **1994**, *1186*, 19−26.
(13) Faxén, K.; Gilderson, G.; Ädelroth, P.; Brzezinski, P. *Nature* **2005**, *437*, 286−289.
(14) Belevich, I.; Verkhovsky, M. I.; Wikström, M. *Nature* **2006**, *440*, 829−832.
(15) Hosler, J. P.; Ferguson-Miller, S.; Mills, D. A. *Annu. Rev. Biochem.* **2006**, *75*, 165−187.
(16) Gibson, Q. H.; Greenwood, C. *Biochem. J.* **1963**, *86*, 541−554.
(17) Chance, B.; Erecinska, M. *Arch. Biochem. Biophys.* **1971**, *143*, 675−687.
(18) Dyer, R. B.; Einarsdóttir, O.; Killough, P. M.; López-Garriga, J. J.; Woodruff, W. H. *J. Am. Chem. Soc.* **1989**, *111*, 7657−7659.
(19) Einarsdóttir, O.; Dyer, R. B.; Lemon, D. D.; Killough, P. M.; Hubig, S. M.; Atherton, S. J.; López-Garriga, J. J.; Palmer, G.; Woodruff, W. H. *Biochemistry* **1993**, *32*, 12013−12024.
(20) Brändén, M.; Sigurdson, H.; Namslauer, A.; Gennis, R.; Ädelroth, P.; Brzezinski, P. *Proc. Natl. Acad. Sci. U.S.A.* **2001**, *98*, 5013−5018.

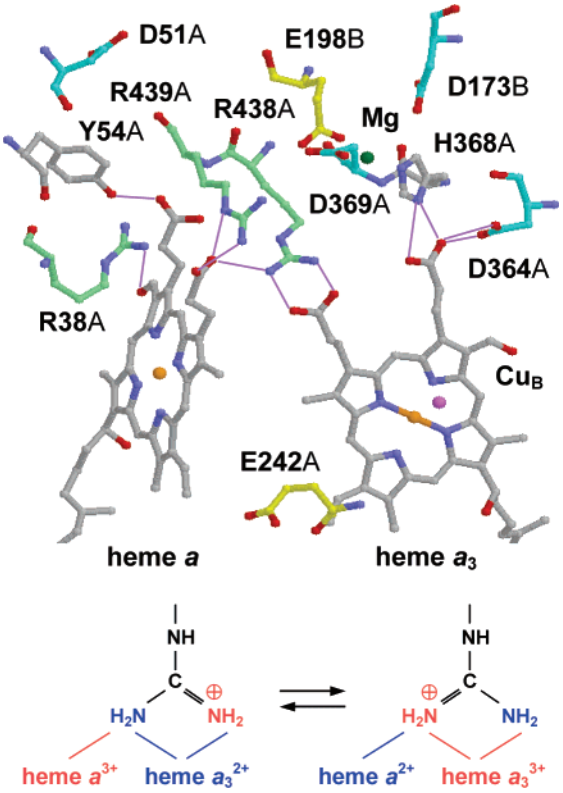

Figure 1. Structure of bovine C*c*O. The diagram was extracted from coordinates in PDB file 2OCC[2] of fully oxidized bovine C*c*O. Residues around the heme propionates and Mg^{2+} are shown, together with Asp-51 and Glu-242. A or B labels indicate residues of subunit I or II. Carbon atoms of Arg, Asp, and Glu residues are plotted in green, cyan, and yellow. Purple lines indicate close contact (less than 3.2 Å) between oxygen atoms of propionate groups and amino acid head groups. The lower panel is a schematic of suggested charge reorganization of the protonated guanidinium group of Arg-438 when interacting with the $a^{3+}a_3^{2+}$ (left) and $a^{2+}a_3^{3+}$ (right) states.

to millisecond range, has provided valuable information on the kinetics of electron transfer, proton uptake and release, and electrogenic events of proton movement. However, the method has not yet been adaptable to IR spectroscopy so that direct observation of the protonatable groups involved has not been possible. The reverse reaction of electron transfer from heme a_3 to heme *a* can be initiated by photolysis of CO from the mixed valence (MV) (i.e., heme a_3 and Cu_B reduced) state,[23,24] and this reaction has been studied by rapid transient vis/UV,[25−29] Raman,[30] electrometric,[31] and photoacoustic[32] methods. In this case, IR methods can also be applied, in particular by studying the static photolysis spectrum under continuous illumination[33−36] or the transient spectrum after laser excitation.[37] In bovine C*c*O, this reversed electron transfer has a pH-independent component with rate constants of 1.2 ns[29] and 3 μs[27,38] that causes around 30% reversed electron transfer to heme *a* from heme a_3.[27] An additional phase of reversed electron transfer occurs at high pH with millisecond kinetics.[27] In C*c*O from *Paracoccus denitrificans* and *Rhodobacter sphaeroides*, the pH-independent phase is larger, resulting in 50%[31] and 45−100%[27,39] reversed electron transfer, respectively, presumably because of different operative midpoint potentials. In this study, the MV−CO (−CO indicates with CO bound) photolysis approach was used in combination with attenuated total reflectance Fourier transform infrared (ATR-FTIR) methods to further study the IR changes associated with reversed electron transfer in bovine C*c*O, with emphasis on proton-related changes. Data are discussed in relation to the mechanism of heme−heme electron transfer and its linkage to proton rearrangements.

Materials and Methods

Sample Handling. Samples were prepared essentially as described previously. In brief, "fast" C*c*O was purified from beef heart[40] and prepared as detergent-free "ATR-ready" material.[41,42] An ATR-ready sample was deposited as a stable film on the ATR prism (3 mm diameter silicon, three-bounce, SensIR). After rehydration with buffer, the sample was covered with a perfusion chamber.[43] To ensure that the C*c*O would be in the fast oxidized state[44] when reoxidized, the protein film was first reduced with 3 mM sodium dithionite.[41,42] Buffers used were 100 mM potassium phosphate, 100 mM KCl at pH 6.0 and 7.0, 50 mM phosphate, 50 mM Tris, 100 mM KCl at pH 8.5, 50 mM phosphate, and 50 mM CHES, 100 mM KCl at pH 9.0 and 9.8. Anaerobic conditions were maintained by addition of glucose (20 mM), catalase (20 μg/mL), and glucose oxidase (100 μg/mL) to 5 mL of degassed buffer solution just before it was injected into the ATR chamber. For measurements after H/D exchange, D_2O buffers were prepared by assuming $pD = pH_{reading} + 0.4$[45] and used for preparation of ATR-ready materials and all subsequent manipulations.

Preparation of the MV−CO Form. To prepare the MV−CO state, the prereduced enzyme was reoxidized by replacing the dithionite with an anaerobic buffer containing 0.5 mM ferricyanide, followed by anaerobic buffer containing CO gas. A 10−40 min period was allowed for formation of the MV−CO compound, after which time light/dark cycles of CO photolysis/recombination were started. As these cycles progressed, the sample slowly accumulated an increasing fraction of the FR−CO form due to further reduction by CO in the light. However,

(21) Verkhovsky, M. I.; Jasaitis, A.; Verkhovskaya, M. L.; Morgan, J. E.; Wikström, M. *Nature* **1999**, *400*, 480−483.
(22) Verkhovsky, M. I.; Morgan, J. E.; Puustinen, A.; Wikström, M. *Nature* **1996**, *380*, 268−270.
(23) Boelens, R.; Wever, R. *Biochim. Biophys. Acta* **1979**, *547*, 296−310.
(24) Brzezinski, P.; Malmström, B. G. *Biochim. Biophys. Acta* **1987**, *894*, 29−38.
(25) Oliveberg, M.; Malmström, B. G. *Biochemistry* **1991**, *30*, 7053−7057.
(26) Verkhovsky, M. I.; Morgan, J. E.; Wikström, M. *Biochemistry* **1992**, *31*, 11860−11863.
(27) Brändén, M.; Namslauer, A.; Hansson, Ö.; Aasa, R.; Brzezinski, P. *Biochemistry* **2003**, *42*, 13178−13184.
(28) Ädelroth, P.; Sigurdson, H.; Hallén, S.; Brzezinski, P. *Proc. Natl. Acad. Sci. U.S.A.* **1996**, *93*, 12292−12297.
(29) Pilet, E.; Jasaitis, A.; Liebl, U.; Vos, M. H. *Proc. Natl. Acad. Sci. U.S.A.* **2004**, *101*, 16198−16203.
(30) Ji, H.; Yeh, S. R.; Rousseau, D. L. *J. Biol. Chem.* **2004**, *279*, 9392−9399.
(31) Belevich, I.; Tuukkanen, A.; Wikström, M.; Verkhovsky, M. I. *Biochemistry* **2006**, *45*, 4000−4006.
(32) Larsen, R. W. *Photochem. Photobiol. Sci.* **2006**, *5*, 603−610.
(33) Hellwig, P.; Rost, B.; Mäntele, W. *Spectrochim. Acta, A* **2001**, *57*, 1123−1131.
(34) Rost, B.; Behr, J.; Hellwig, P.; Richter, O. M. H.; Ludwig, B.; Michel, H.; Mäntele, W. *Biochemistry* **1999**, *38*, 7565−7571.
(35) Okuno, D.; Iwase, T.; Shinzawa-Itoh, K.; Yoshikawa, S.; Kitagawa, T. *J. Am. Chem. Soc.* **2003**, *125*, 7209−7218.
(36) McMahon, B. H.; Fabian, M.; Tomson, F.; Causgrove, T. P.; Bailey, J. A.; Rein, F. N.; Dyer, R. B.; Palmer, G.; Gennis, R. B.; Woodruff, W. H. *Biochim. Biophys. Acta* **2004**, *1655*, 321−331.
(37) Nyquist, R. M.; Heitbrink, D.; Bolwien, C.; Gennis, R. B.; Heberle, J. *Proc. Natl. Acad. Sci. U.S.A.* **2003**, *100*, 8715−8720.
(38) Morgan, J. E.; Verkhovsky, M. I.; Puustinen, A.; Wikström, M. *Biochemistry* **1993**, *32*, 11413−11418.
(39) Ädelroth, P.; Brzezinski, P.; Malmström, B. G. *Biochemistry* **1995**, *34*, 2844−2849.
(40) Moody, A. J.; Cooper, C. E.; Rich, P. R. *Biochim. Biophys. Acta* **1991**, *1059*, 189−207.
(41) Iwaki, M.; Puustinen, A.; Wikström, M.; Rich, P. R. *Biochemistry* **2003**, *42*, 8809−8817.
(42) Iwaki, M.; Puustinen, A.; Wikström, M.; Rich, P. R. *Biochemistry* **2004**, *43*, 14370−14378.
(43) Rich, P. R.; Breton, J. *Biochemistry* **2002**, *41*, 967−973.
(44) Moody, A. J. *Biochim. Biophys. Acta* **1996**, *1276*, 6−20.
(45) Glasoe, P. K.; Long, F. A. *J. Phys. Chem.* **1960**, *64*, 188−190.

the FR−CO contribution to the photolysis spectra could be accurately assessed and subtracted by monitoring the frequency of the bound CO, which moved progressively from 1965 cm^{-1} in the pure MV−CO form toward the 1963 cm^{-1} position of the FR form, and runs were terminated when it had drifted below 1964 cm^{-1}. The MV state could be regenerated several times by repeating the dithionite reduction and reoxidation sequence to allow further data acquisition. In a typical run, 50−75 photolysis cycles were averaged, after which time the FR form had accumulated to around 35%, and the pure MV state was regenerated 3−4 times.

Preparation of the FR−CO Form. The FR−CO state of samples used for MV−CO photolysis measurements was generated with anaerobic buffer containing 3 mM dithionite and CO gas. The FR−CO form is characterized by a CO band around 1963 cm^{-1} arising from the principal α form together with two broader β forms.[46−48] The FR−CO state was sufficiently stable that many hundreds of photolysis cycles could be performed on a single sample.

IR Difference Spectra. ATR-FTIR spectra were recorded in room light and at room temperature with a Bruker ISF 66/S spectrometer, fitted with a liquid nitrogen-cooled MCT-A detector. Spectral resolution was 4 cm^{-1}, and cited frequencies have an accuracy of ±1 cm^{-1}. IR photolysis difference spectra were measured essentially as described previously.[49] Actinic illumination was provided by a 250 W tungsten halogen lamp. The beam was filtered through 10 cm of water, glass heat filters, and a BG39 580 nm short-pass filter and delivered to the sample via fiber optics. Typically, 100 interferograms were averaged over 13 s as a background in darkness, the actinic beam was switched on, and 100 interferograms were averaged to produce a light *minus* dark difference spectrum. The cycles were repeated after 15 s of dark relaxation. Spectra were averaged in groups of 25 so that the stability and, in the MV−CO form, the extent of conversion to the FR−CO state could be assessed. The photolysis spectra also contained a broad baseline shift due to heating during illumination. To measure the heating effect, the same light/dark cycles were performed on aerobic samples that had been oxidized with 0.5 mM ferricyanide and in which no photolysis can occur. Spectra shown are averages of 200−300 cycles after subtraction of this heating baseline shift and, in the case of the MV−CO form, after removal of any contribution from the FR−CO form.

Results

Comparison of FR−CO and MV−CO Photolysis Spectra. The photolysis spectra at 1985−1940 and 1780−1000 cm^{-1} of FR−CO and MV−CO forms are compared in Figure 2. The spectra have been normalized so that the intensities of bands due to photolysis of bound CO at 1965 or 1963 cm^{-1} are equal and, therefore, the spectra represent roughly comparable extents of CO photolysis. The spectra are in agreement with prior published work on bovine C*c*O[35,36,48−50] and are very similar to equivalent data from bacterial systems.[34,51,50] As expected, the major CO band is close to 1963 cm^{-1} in the FR−CO data, but is shifted to 1965 cm^{-1} in the MV form,[35,36] and this provided the means of deconvoluting pure photolysis spectra of the MV−CO form in the FR−CO/MV−CO mixtures that accumulate during photolysis cycles (see the Materials and Methods). All signals in the FR−CO spectra were pH-independent between pH 6 and pH 9.8 (see the Supporting Information, Figure S1), again consistent with published data.[35,49] In contrast, the photolysis spectra of the MV−CO form have a marked pH/D dependency in the 1780−1000 cm^{-1} range above pH/D 8,[36] most easily seen as a marked increase in the intensities of most bands (Figure 3).

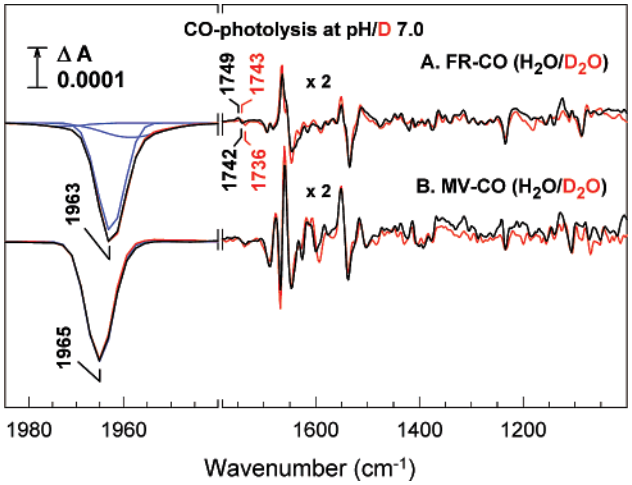

Figure 2. ATR-FTIR photolysis spectra of FR−CO and MV−CO forms of C*c*O. Light minus dark ATR-FTIR difference spectra are shown for the FR−CO form (trace A in H_2O (black) and D_2O (red) media) and MV−CO form (trace B in H_2O (black) and D_2O (red) media) at pH/D 7.0. The left panel shows the IR bands of photolyzed CO, and the right panel shows the IR changes in protein and heme. Amplitudes have been normalized to give the same maximum intensities of the negative CO bands, and baseline shifts and FR−CO contributions to the MV−CO spectra have been subtracted. Deconvoluted Gaussian components of the CO bands are overlaid (blue). Frequencies and bandwidths: for the FR−CO state, 1958.5 cm^{-1} and 14.1 cm^{-1}, 1962.7 cm^{-1} and 6.7 cm^{-1}, 1973.0 cm^{-1} and 10.7 cm^{-1}; for the MV−CO state, 1965.0 cm^{-1} and 6.8 cm^{-1} (this simulated component exactly overlies the experimental trace and so is not visible). The right panel data are expanded 2-fold compared to those in the left panel.

Discussion

Photolysis Spectra of FR−CO C*c*O. IR photolysis spectra of the FR−CO state from various sources in the 2000−1000 cm^{-1} range have already been reported,[34−36,48−51] and only details relevant to the analysis of the MV−CO photolysis data are discussed here. The band of bound CO in bovine C*c*O is close to 1963 cm^{-1}. However, this always comprises a dominating α form and several broader β forms.[46−48,52] These were deconvoluted as three Gaussian components (blue overlays on the Figure 2A spectrum): an α form (1962.7 cm^{-1}, bandwidth approximately 7 cm^{-1}) and two β forms (1958 and 1973 cm^{-1}, bandwidths of 14 and 11 cm^{-1}, respectively). Their peak positions and ratios were independent of pH and H/D exchange[46,48,49] as were the spectra in the 1800−1000 cm^{-1} range (see the Supporting Information, Figure S1). Although two major forms of heme-bound CO that are in a pH-dependent equilibrium have been reported in FR−CO C*c*O of *Rb. sphaeroides*[53,54] and *P. denitrificans*,[34] these data have not been observed consistently and may arise from preparation-dependent alterations.

Changes that arise from protein and cofactors in the 1800−1000 cm^{-1} region that are associated with CO photolysis have

(46) Einarsdóttir, O.; Choc, M. G.; Weldon, S.; Caughey, W. S. *J. Biol. Chem.* **1988**, *263*, 13641−13654.
(47) Park, S.; Pan, L. P.; Chan, S. I.; Alben, J. O. *Biophys. J.* **1996**, *71*, 1036−1047.
(48) Iwase, T.; Varotsis, C.; Shinzawa-Itoh, K.; Yoshikawa, S.; Kitagawa, T. *J. Am. Chem. Soc.* **1999**, *121*, 1415−1416.
(49) Rich, P. R.; Breton, J. *Biochemistry* **2001**, *40*, 6441−6449.
(50) Heitbrink, D.; Sigurdson, H.; Bolwien, C.; Brzezinski, P.; Heberle, J. *Biophys. J.* **2002**, *82*, 1−10.
(51) Puustinen, A.; Bailey, J. A.; Dyer, R. B.; Mecklenburg, S. L.; Wikström, M.; Woodruff, W. H. *Biochemistry* **1997**, *36*, 13195−13200.
(52) Caughey, W. S.; Dong, A.; Sampath, V.; Yoshikawa, S.; Zhao, X. J. *J. Bioenerg. Biomembr.* **1993**, *25*, 81−91.
(53) Mitchell, D. M.; Shapleigh, J. P.; Archer, A. M.; Alben, J. O.; Gennis, R. B. *Biochemistry* **1996**, *35*, 9446−9450.
(54) Wang, J.; Takahashi, S.; Hosler, J. P.; Mitchell, D. M.; Ferguson-Miller, S.; Gennis, R. B.; Rousseau, D. L. *Biochemistry* **1995**, *34*, 9819−9825.

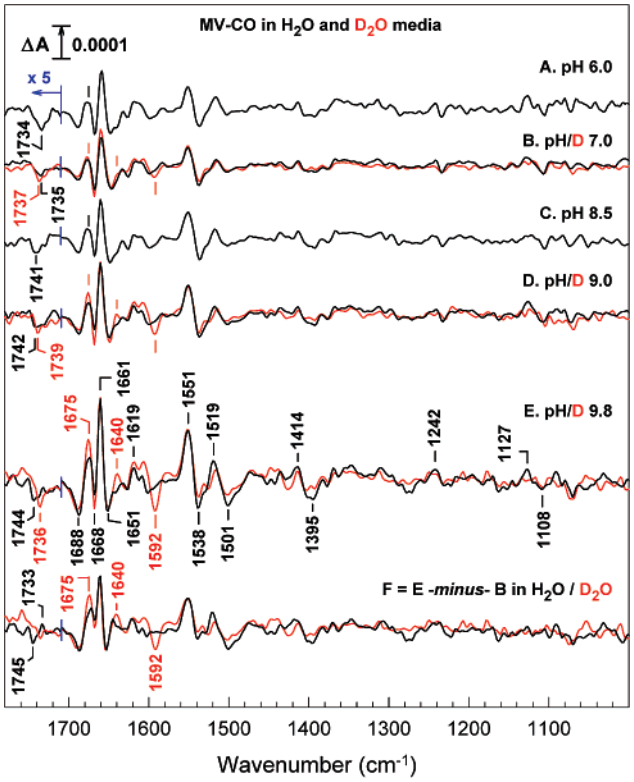

Figure 3. ATR-FTIR photolysis spectra of the MV−CO form of C*c*O. Light minus dark ATR-FTIR difference spectra were measured at pH 6.0 (trace A), 7.0 (trace B, data of Figure 2B), 8.5 (trace C), 9.0 (trace D), and 9.8 (trace E) in H_2O media (black) and at pD 7.0 (trace B, data of Figure 2B), 9.0 (trace D), and 9.8 (trace E) in D_2O media (red). Typically, the final raw spectra were averages from 200−300 dark/light cycles (i.e., 20000−30000 interferograms in total). Amplitudes have been normalized to give the same maximum intensities of the negative CO bands, and baseline shifts and FR−CO contributions have been subtracted. The pH-dependent phase alone (trace F) was calculated by subtraction of the photolysis spectrum at pH 9.8 minus that at pH 7 (E minus B, H_2O data, black) and that at pD 9.8 minus that at pD 7 (E minus B, D_2O data, red).

also been well documented[34−36,48−51] though are not yet well assigned. However, it seems clear that the spectra are dominated by shifts of heme a_3 and its ligands together, possibly, with ligands of Cu_B. This is true even in the 1550−1500 cm^{-1} region where changes are usually dominated by amide II band shifts; in this case the lack of a large effect of H/D exchange (Figure 2, data overlaid on trace A) is due to domination by heme, rather than amide II, band shifts. Of particular note is a peak/trough at 1749/1742 cm^{-1} that had been reasonably attributed initially to an upshift of the ν(C═O) of the protonated form of Glu-242, a conserved glutamic acid in subunit I (Figure 1),[18,48] on the basis of the effect of replacement of the equivalent residue in *Escherichia coli* cytochrome *bo* on a similar band shift in its FR−CO photolysis spectrum.[51] However, H/D exchange had a more complex effect than the uniform 3−6 cm^{-1} downshift expected for a single carboxylic component, and this suggested that the changes arise from several components,[49] a conclusion that has been supported recently.[35] Furthermore, changes in this region in equivalent CO photolysis spectra in closely related C*c*Os from different sources are more varied than might have been expected if this highly conserved residue were the sole source of the shift: whereas photolysis of the FR−CO form of cytochrome *bo* from *E. coli* in D_2O[51] does result in a peak/trough at 1731/1724 cm^{-1}, no clear equivalent band shifts could be observed in photolysis spectra of the FR−CO forms of *P. denitrificans*[34] or *Rb. sphaeroides*[50] C*c*Os. Given these inconsistencies, assignment of the carboxylic signal in bovine FR−CO photolysis spectra solely to perturbation of Glu-242 is questionable. It might be noted that assignment to Asp-51 is also unlikely because the residue in the atomic model of the FR form is exposed to solvent and, therefore, deprotonated in the FR (and presumably the FR−CO) state.[4]

Photolysis Spectra of the MV CO State. Deconvolution of Spectra Due Solely to Heme−Heme Electron Transfer. The MV−CO photolysis spectra are composed of changes caused by dissociation of CO from heme a_3 iron together with changes arising from reversed electron transfer from heme a_3 to heme *a*. In the data of Figure 3, the photolyzed CO bands of all spectra have been normalized so that they represent the same extents of CO photolysis. The increasing intensity of spectra above pH 8 is then due solely to the increased extent of reversed electron transfer from heme a_3 to heme *a*.[27,55,56] Hence, subtraction of data at pH/D 7.0 (trace B) from data at pH/D 9.8 (trace E) should represent the difference spectra that are solely due to the pH-dependent component of reversed electron transfer.[36] These double difference spectra are overlaid in Figure 3F. The major features are relatively unaffected by H/D exchange because they arise from amide I or redox-dependent bands of the hemes and their ring substituents. For example, the positive band at 1661 cm^{-1} is an amide I change that is linked to the redox state of heme *a*.[57] However, the formyl groups of hemes *a* and a_3 have strong redox-sensitive bands in the amide I region[58,59] and should also contribute. McMahon et al.[36] have assigned the 1620/1650 cm^{-1} peak/trough to the formyl group of heme *a* and the 1675/1667 cm^{-1} peak/trough to the formyl group of heme a_3. Although the 1550−1500 cm^{-1} region is usually dominated by amide II changes, the lack of a large effect of H/D exchange in Figure 3 shows that this is not the case in the MV−CO photolysis spectra. Instead, the positive bands at 1551 and 1519 cm^{-1} are most likely primarily ring modes of ferrous heme *a* and the troughs at 1538 and 1501 cm^{-1} loss of the corresponding ring modes of ferrous heme a_3. This is in part consistent with data that link the positive band at 1551 cm^{-1} to ferrous heme *a*.[43,57] Other band changes around 1414(+)/1395(−), 1242(+), 1127(+), and 1108(−) cm^{-1} that are evident in the photolysis spectra (traces A−E) are very likely to be heme or heme−histidine bands, but these are less apparent in the pH-dependent heme−heme spectra (traces F) probably because of cancellation due to opposite redox changes of the hemes.

Photolysis Spectra of the MV CO State. pH Effects. In contrast to the heterogeneous band of bound CO in bovine C*c*O, the equivalent band in photolysis spectra of MV−CO C*c*O can be simulated as a single Gaussian component at 1965 ± 0.2 cm^{-1} with a bandwidth of 6.8 ± 0.2 cm^{-1} (Figure 2B, a blue line that is almost exactly overlaid by the experimental data), and equivalents of the FR−CO β forms were absent. This demonstrates definitively that the β forms are aberrant in their

(55) Ädelroth, P.; Sigurdson, H.; Hallen, S.; Brzezinski, P. *Proc. Natl. Acad. Sci. U.S.A.* **1997**, *93*, 12292−12297.
(56) Hallén, S.; Brzezinski, P.; Malmström, B. G. *Biochemistry* **1994**, *33*, 1467−1472.
(57) Gorbikova, E. A.; Vuorilehto, K.; Wikström, M.; Verkhovsky, M. I. *Biochemistry* **2006**, *45*, 5641−5649.
(58) Callahan, P. M.; Babcock, G. T. *Biochemistry* **1983**, *22*, 452−461.
(59) Woodruff, W. H.; Dallinger, R. F.; Antalis, T. M.; Palmer, G. *Biochemistry* **1981**, *20*, 1332−1338.

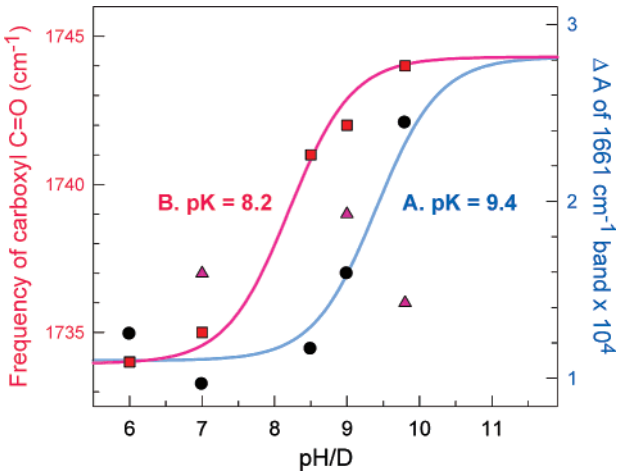

Figure 4. pH titrations of the intensity of the 1661 cm^{-1} band and the frequency of carboxyl the C=O stretch in MV−CO photolysis spectra. Data are taken from the MV−CO photolysis spectra of Figure 3. Intensities at 1661 cm^{-1} (right axis) are plotted against measured pH (black circles) and fitted with a theoretical curve of pK = 9.4 (blue) that is based on an extrapolated maximum of 100% reversed electron transfer from heme a_3. Frequencies of the carboxylic acid trough around 1740 cm^{-1} (left axis) are plotted in H_2O (red squares) and D_2O (pink triangles) media, and a theoretical curve of pK = 8.2 (red) is overlaid.

reactivity with CO, and most probably with other ligands, consistent with the finding that they are unable to react with CO/O_2 to form the P_M intermediate. Whether the frequency of the CO band in bovine MV−CO C*c*O is pH-dependent is controversial,[35,36] and resolution is not straightforward because of contamination of the MV−CO spectra with variable amounts of the FR−CO form that tend to interfere more at higher pH values. Our data confirm the reported shift to lower frequencies at high pH,[36] but subtraction of the variable contribution of the FR−CO form always yielded a single Gaussian component of constant frequency (1965 cm^{-1}) and bandwidth (6.8 cm^{-1}), showing convincingly that the peak position is pH-independent throughout the pH range 6−9.8, in agreement with Okuno et al.[35]

The Figure 3 data (normalized to equal extents of CO photolysis) do however confirm the reported pD dependencies of these photolysis spectra in the 1780−1000 cm^{-1} range[36] and show the same effect in H_2O media. The larger IR perturbations above pH/D 8 arise from the known increased extent of reversed electron transfer.[27] This pH/D dependency was quantitated from a plot of the size of the positive band at 1661 cm^{-1} versus pH (Figure 4, right axis). Its extent continued to increase up to pH 9.8, the highest pH for which reliable, stable formation of the MV−CO state was possible and fitting of a unique Henderson−Hasselbach curve to determine pK was not possible. However, using estimated extents of reversed electron transfer of 30% for the pH-independent phase[27] and 20% for the pH-dependent phase at pH 9,[55] the extrapolated value of $\Delta A_{1661\ cm^{-1}}$ for 100% reversed electron transfer would be 2.8×10^{-4}, giving an apparent pK of 9.4 (Figure 4A). Although this does not put an upper limit on the pK of the protonatable group itself since it might continue to titrate after the extent of reversed electron transfer has maximized, the pK is consistent with estimated values for the pK of the millisecond reversed-electron-transfer phase observed in the visible region[55,56] and could be consistent with IR data in D_2O[36] where, despite fitting of a nominal pK(in D_2O) of 7.6−7.9, sufficiently high pD values to saturate the process may not have been achieved. Since the effect is associated with an increased extent of electron transfer from heme a_3 to heme a, it must arise from a redox-linked protonatable group.

A second, more subtle effect of pH is evident in the 1750−1730 cm^{-1} region of these MV−CO photolysis spectra (shown expanded in Figure 2). It is well-known that bovine C*c*O spectra exhibit predominantly a trough in this region in both H_2O[35] and D_2O[35,36] media that has been assigned to a carboxylic acid that either deprotonates or has an extinction coefficient decrease. Its amplitude remained roughly constant over the measured range of pH(D) values, indicating that the change is associated with CO photolysis from heme a_3 iron or with the pH-independent component of the reversed electron transfer. In contrast to the inconsistencies between carboxylic acid bands in FR−CO photolysis spectra of C*c*O from different sources discussed above, equivalent MV−CO photolysis spectra show more consistency: *P. denitrificans* C*c*O spectra have a H/D-sensitive 1746 cm^{-1} trough at pH/D 7,[34] and *Rb. sphaeroides* C*c*O spectra exhibit a 1745 cm^{-1} trough at pH 8.5.[37] What has not been noted previously, however, is the fact that its frequency in bovine MV−CO photolysis spectra in H_2O media shifts from 1734 cm^{-1} at pH 6 to 1744 cm^{-1} at pH 9.8 and with an $n = 1$ pK of 8.2 (Figure 4B). This effect has not been observed previously because only effects of pD in D_2O media have been reported to date[36] and, as discussed below, the effect of pD is more complex and difficult to detect. Such upshifts of the carboxylic ν(C=O) band are most likely caused by altered hydrogen bonding, with frequency decreasing as the strength of hydrogen bonding increases. Hence, it seems likely that this effect is caused by a titratable group with a pK of 8.2 whose deprotonation at high pH leads to a more weakly hydrogen bonded state of the IR-active carboxylic group. D_2O causes a downshift at high pH as expected for a protonated carboxylic acid, but causes an upshift at low pH (compare data in Figure 4). Such upshifts in D_2O have been explained previously in terms of the deuteration of a group that is strongly hydrogen bonded to the observable carboxylic group;[35] the unusual D_2O shift pattern in the present data could be consistent with the above proposal of a titratable group that hydrogen bonds to the IR-observable carboxylic acid when in its deuterated state at lower pH/D values. Its pK of 8.2 is too low for it to be the same as the group that controls the extent of the pH-dependent phase of electron transfer.

One further striking effect of pH/pD was evident in the spectra of Figure 3F, namely, the appearance of a prominent trough at 1592 cm^{-1} in D_2O. This H/D-induced 1592 cm^{-1} trough is also evident in the CO photolysis data themselves (traces B, D, and E) and increased at higher pD values. The guanidinium group of arginine has a pK_a of 12.48 and so is likely to remain protonated unless placed in an extreme environment. Its protonated state has a pair of strong $\nu_{as}(CN_3H_5^+)$ and ν_s-$(CN_3H_5^+)$ bands at 1672 and 1632 cm^{-1}, respectively, that downshift to 1611 and 1585 cm^{-1} in D_2O.[60] These assignments were confirmed by isotope shifts in $^{15}N_2$-guanidinium-labeled arginine (see the Supporting Information, Figure S2). In the spectra of pH-dependent reversed electron transfer (Figure 2F), comparison of the spectra in H_2O and D_2O reveals two decreases in the H_2O spectrum at 1675 and 1640 cm^{-1} relative to the

(60) Barth, A. *Prog. Biophys. Mol. Biol.* **2000**, *74*, 141−173.

D_2O spectrum that are replaced by at least one trough at 1592 cm^{-1} in the D_2O spectrum. This is strongly indicative of an arginine residue, which either deprotonates or undergoes an environmental or conformational change that shifts its $\nu_{as}(CN_3H_5^+)$ and $\nu_s(CN_3H_5^+)$ band frequencies.

Structural and Functional Implications of IR Changes. The lack of pH dependencies of the bands of bound CO in both FR and MV states indicates that none of the protonatable groups that are close enough to bound CO to directly affect its binding, namely, Tyr-244, His-376 (proximal ligand to a_3), or His-290 or His-291 (Cu_B ligands), can have p*K* values in the 6−9.8 range in the MV−CO or FR−CO states as any protonation state change should affect the CO stretch band. This is consistent with the lack of proton exchange with the external medium when CO is ligated to either form and is a reflection of the strong conservation of zero net charge change within the binuclear center.[11,12]

Electron transfer from heme *a* to the binuclear center is a key component of many current models of coupled proton translocation, and the IR spectra can also provide information on changes in cofactors and amino acids, including protonation changes that are not measurable by other methods. Heme $a \rightarrow a_3$ forward electron transfer has not yet been amenable to IR analyses, and the protonation changes have remained unresolved. However, IR spectra of the reverse $a_3 \rightarrow a$ reaction can be observed by photolysis of the MV−CO state, and *provided that the protonation pattern of the MV state immediately after CO photolysis of the MV−CO form is identical to that of the MV state formed during catalysis*, the protonation changes should also be the reverse of those in the forward catalytic direction. This point has not been addressed to date, but is critical to data interpretations. It has been proposed that a proton originating from the N phase moves in concert with heme $a \rightarrow a_3$ electron transfer onto a trap site where it can minimize the energy penalty of the negative charge arriving on heme a_3.[10] Subsequent protonation of an oxygen intermediate causes repulsion of the trap proton into the P phase, completing the proton-motive sequence. This model requires that the mixed valence state should have two protons in positions that allow them to charge-counterbalance the two electronic charges on heme a_3 and Cu_B, as is known to be the case.[11] There is general agreement that the first of these is bound into the singly reduced binuclear center via the K channel,[20] most probably forming water from a hydroxide ligand on Cu_B.[61] The location of the second proton is less certain: it should initially reside on the trap site to counterbalance the introduction of the second electron into the binuclear center. This trap proton should be repelled into the P phase when the doubly reduced binuclear center takes up a further proton into the oxygen-reactive site. Whether this occurs before or after reaction with oxygen might depend on the pH, particularly since it has been shown that the distal ligand of ferric heme a_3 is water/hydroxide with a p*K* of 9.[27] Hence, proton uptake onto ferric a_3-OH^- (and hence trap deprotonation) could occur before reaction with oxygen at high pH, but at lower pH proton uptake into the binuclear center and trap deprotonation might have to await creation of a protonation site by the oxygen chemistry unless a further protonation site is available within the binuclear center. One corollary of this reasoning is that both pH-dependent and pH-independent phases of reversed electron transfer should be associated with a reversed electrogenic component. This contrasts with the report of Jasaitis et al.[62] that $a_3 \rightarrow a$ reversed electron transfer is nonelectrogenic, although this study was carried out only at pH 7 where the electrogenic protonation exchange between trap and other internal site(s) may have been hidden by an additional electrogenic heme $a \rightarrow Cu_A$ reaction. At high pH, a much larger electrogenic phase associated with heme a_3 oxidation is predicted as water deprotonates via the K channel,[27] and this remains to be tested. A more revealing case is photolysis of CO from the MV−CO form followed by reaction with oxygen to produce the P_M state: Even at low pH, if the second proton were on the trap site, this reaction should lead to binuclear center protonation and trap deprotonation, both of which should be electrogenic. This reaction, however, is not electrogenic,[62] and so it appears that the MV−CO state must have two protons bound within the binuclear center with the trap deprotonated, even at low pH (despite calculations suggesting that this is unlikely[61]), and that this is also the case for the natural MV state formed during catalysis. At very high pH, it appears that an additional protonation site is created by conversion of the distal water ligand of heme a_3 to hydroxide[27] though whether this species, which might contravene the otherwise strictly electroneutral changes of the stable binuclear center intermediates,[10] is relevant to the natural catalytic cycle is questionable.

Most clear of the pH-dependent effects that are evident in the MV−CO photolysis data is the well-known pH dependency of the magnitude of the 1780−1000 cm^{-1} changes that arise from the increased extent of electron transfer from heme a_3 to heme *a* at higher pH.[27,55,56] This effect must be caused by a titratable group whose protonation state affects the redox potential of heme a_3 and/or heme *a*. The atomic structures[1−4] reveal many potential redox-linked protonatable groups, including the heme propionates, the histidine and water ligands to the hemes and Cu_B, protonatable groups in the K and D channels, and a cluster of groups "above" the heme propionates and around the bound Mg^{2+} (Figure 1). However, there are few IR signatures in the data that are characteristic of a changing protonation state.[63] The 1742 cm^{-1} trough arising from a carboxylic group is associated only with the pH-independent processes, and the group that influences its frequency has too low a p*K*. The only other amino acid signatures that might be relevant are the bands in Figure 3 that we have assigned to arginine. Given that the arginine bands arise from reorientation rather than deprotonation (generally considered unlikely because of its very high solution p*K*), a different group must be responsible for the pH dependency of the reversed-electron-transfer extent. It seems most likely that the effect is caused by the distal water ligand of ferric heme a_3, which has been shown by EPR spectroscopy to have a p*K* of around 9.[27] Formation of a hydroxide ligand will lower the heme a_3 midpoint potential and hence increase the extent of reversed electron transfer as observed. The heme $a_3^{3+}-OH^-$ is at 450 cm^{-1} in Raman data[64,65] and will not appear in the IR spectra reported here. Some support for these interpretations comes from Song et al.,[61]

(61) Song, Y.; Michonova-Alexova, E.; Gunner, M. R. *Biochemistry* **2006**, *45*, 7959−7975.
(62) Jasaitis, A.; Verkhovsky, M. I.; Morgan, J. E.; Verkhovskaya, M. L.; Wikström, M. *Biochemistry* **1999**, *38*, 2697−2706.
(63) Rich, P. R.; Iwaki, M. In *Biophysical and Structural Aspects of Bioenergetics*; Wikström, M., Ed.; Royal Society of Chemistry: Cambridge, U.K., 2005; pp 314−333.
(64) Han, S.; Ching, Y.; Rousseau, D. L. *Nature* **1990**, *348*, 89−90.

who have calculated that neither the heme propionates nor the heme-associated arginines would have an appropriate p*K* shift, although some outcomes of these calculations contrast with other mechanistic simulations,[66] the known p*K* of the water ligand of heme a_3,[27] the observed uptake of two protons by the MV form at pH 6−8.5,[11] and IR data that suggest at least one accessible heme propionate p*K*.[67,68]

The carboxylic acid signal associated with the pH-independent processes is a separate effect. Given that one or more carboxylic acid groups are sensitive to CO photolysis in the FR−CO state (at least in bovine C*c*O), it is reasonable to expect that at least part of the effect in MV−CO also arises from the CO photolysis itself and involving the same residues. However, the pH-independent electron transfer should also induce some internal proton rearrangements to minimize the energy of the electron transfer even though there is no net proton exchange with the medium. An equivalent trough is present in photolysis spectra of MV−CO forms of bacterial C*c*Os, and in these cases mutagenesis studies indicate assignment to deprotonation of Glu-242.[35−37] In the bovine case, however, where reduction of heme *a* is linked to at least two carboxylic acid deprotonations,[35,43,69] an additional involvement of Asp-51 is possible, since it is buried in the protein and likely to be protonated even at high pH when heme *a* is oxidized.[4,70] In fact, the data in Figure 3 rather suggest that the pH sensitivity of its frequency may arise from a change in the distribution of two component species, rather than a uniform shift of one. The group that affects the frequency (or mixture) of the IR-observable carboxylic band-(s) in a pH-dependent manner must have a p*K* of 8.2 even though it does not itself appear in the MV−CO photolysis spectra. It is most likely one of the groups that confers the known E_m/pH dependencies of midpoint potentials of heme *a*.[71−73] The specific groups involved have not been identified experimentally, although the calculations of Song et al.[61] have suggested that at least four rather remote groups, two glutamic acids and two histidines, have p*K* values that will respond weakly to reversed electron transfer.

The other signal of mechanistic relevance revealed by the IR spectra is the guanidinium group of an arginine. Three conserved arginines interact directly with the hemes, Arg-38, Arg-438, and Arg-439 (Figure 1). Possible mechanistic roles for all three of these arginines have been suggested.[1,70,74] A possible arginine IR signal associated with heme−heme electron transfer in D_2O media has already been noted,[36] although its properties are quite different from those of the signals reported here. The guanidinium groups of Arg-439 and Arg-38 are in close contact with heme *a* D-ring propionate and formyl groups, respectively. The guanidinium group of Arg-438 is in close contact with the D-ring propionate groups of both heme a_3 and heme *a* and is most likely sensitive to charge distribution changes in both hemes.[74] By simple reorientation of its charge to be closer to heme a_3 as shown in the lower part of Figure 1, the guanidinium group of Arg-438 can aid electron transfer from heme *a* to heme a_3 in the catalytic cycle, lowering the energy of the transient intermediate by compensating the negative charge arriving on heme a_3.

In summary, therefore, a mechanistic picture emerges as follows: electron transfer to heme *a* is associated with a complex pattern of protonation changes. These consist of carboxylic acid deprotonations, possibly involving the Glu-242 and Asp-51 residues whose possible mechanistic importance has been noted by many groups, together with changes of other protonatable groups that interact with these residues and whose p*K* values influence the E_m/pH dependency of heme *a*. The charge on heme *a* is further stabilized by reorientation of the charge on Arg-438 (or, possibly, net protonation of Arg-438 or one of its neighboring groups), a residue whose likely functional importance has also been emphasized.[1,74,75] Electron transfer to heme a_3 causes relaxation of these effects around heme *a* and orientation of the charge on Arg-438 toward heme a_3. This lowers the cost of introduction of charge into the binuclear center and so is integral to the catalytic mechanism of protonating the trap site. Presumably, the trap site itself then becomes protonated, perhaps with the reoriented Arg-438 providing part of the proton-transfer pathway to it. Regardless of whether Arg-438 is the trap itself, protonatable groups that are redox-linked to *both* heme *a and* the binuclear center are central to the coupling mechanism and indeed have been detected experimentally:[73] The trap begins to protonate with heme *a* reduction, and this aids electron transfer to the binuclear center by lowering the midpoint potentials of binuclear metal sites. Completion of electron transfer to the binuclear center is linked to completion of trap protonation. Subsequent protonation of the binuclear center oxygen-reactive cavity results in trap deprotonation to the P phase. Even at low pH, this appears to precede oxygen reaction in the MV → MV−O_2 → P_M sequence, but may involve nonphysiological protonation of a heme a_3 distal hydroxide at very high pH. It is this group that results in a greater extent of reversed electron transfer observed at very high pH by lowering the heme a_3 midpoint potential. This model, which is consistent with a number of other current models of function, provides a framework to guide further IR studies to elucidate the complex pattern of electron/proton linkages that define the proton-motive mechanism of the C*c*Os.

Acknowledgment. We are grateful to Dr. W. John Ingledew for his kind gift of $^{15}N_2$-labeled arginine and Mr. Santiago Garcia for specialist electronic and mechanical support. This work was funded by a grant from the BBSRC (BB/C51715X/1).

Supporting Information Available: ATR-FTIR difference spectra of FR−CO photolysis of bovine C*c*O at pH/D 6.0−9.8 in the 1840−900 cm^{-1} region and ATR-FTIR spectra of model L-arginine. This material is available free of charge via the Internet at http://pubs.acs.org.

JA067779I

(65) Varotsis, C.; Zhang, Y.; Appelman, E. H.; Babcock, G. T. *Proc. Natl. Acad. Sci. U.S.A.* **1993**, *90*, 237−241.
(66) Siegbahn, P. E. M.; Blomberg, M. R. A.; Blomberg, M. L. *J. Phys. Chem. B* **2003**, *107*, 10946−10955.
(67) Behr, J.; Hellwig, P.; Mäntele, W.; Michel, H. *Biochemistry* **1998**, *37*, 7400−7406.
(68) Behr, J.; Michel, H.; Mäntele, W.; Hellwig, P. *Biochemistry* **2000**, *39*, 1356−1363.
(69) Hellwig, P.; Soulimane, T.; Buse, G.; Mäntele, W. *FEBS Lett.* **1999**, *458*, 83−86.
(70) Yoshikawa, S.; Muramoto, K.; Shinozawa-Itoh, K.; Aoyama, H.; Tsukihara, T.; Shimokata, K.; Katayama, Y.; Shimada, H. *Biochim. Biophys. Acta* **2006**, *1757*, 1110−1116.
(71) Nicholls, P.; Wrigglesworth, J. M. *Ann. N. Y. Acad. Sci.* **1988**, *550*, 59−67.
(72) Wikström, M. K. F.; Krab, K.; Saraste, M. *TIBS* **1982**, *7*, 304−305.
(73) Moody, A. J.; Rich, P. R. *Biochem. Soc. Trans.* **1989**, *17*, 896−897.
(74) Wikström, M.; Ribacka, C.; Molin, M.; Laakkonen, L.; Verkhovsky, M.; Puustinen, A. *Proc. Natl. Acad. Sci. U.S.A.* **2005**, *102*, 10478−10481.
(75) Mills, D. A.; Florens, L.; Hiser, C.; Qian, J.; Ferguson-Miller, S. *Biochim. Biophys. Acta* **2000**, *1458*, 180−187.